MULTIAXIAL FATIGUE CRITERIA FOR AISI 304 AND 2-1/4 Cr–1 Mo STEEL AT 538°C WITH APPLICATIONS TO STRAIN-RANGE PARTITIONING AND LINEAR SUMMATION OF CREEP AND FATIGUE DAMAGE*

J. J. Blass

CONF-820121--1

Abstract

An improved multiaxial fatigue failure criterion was developed based on the results of combined axial-torsional strain cycling tests of AISI 304 and 2-1/4 Cr–1 Mo steel conducted at 538°C (1000°F). The formulation of this criterion involves the shear and normal components of inelastic strain range on the planes of maximum inelastic shear strain range. Optimum values of certain parameters contained in the formulation were obtained for each material by the method of least squares. The ability of this criterion to correlate the test results was compared with that of the usual (Mises) equivalent inelastic strain range criterion. An improved definition of equivalent inelastic strain range resulting from these considerations was used to generalize the theory of Strain Range Partitioning to multiaxial stress-strain conditions and was also applied to the linear summation of creep and fatigue damage. The assessment of these applications of the improved criterion awaits the results of multiaxial creep-fatigue tests currently underway.

CONF-820121--1

DE82 010195

1. Introduction

A number of methods have been proposed for dealing with the problem of creep-fatigue interaction or time-dependent fatigue. Code Case N-47 of the ASME Boiler and Pressure Vessel Code,[1] which governs the design of nuclear power plant components for elevated-temperature service, currently employs a linear summation of cycle and time fractions. Other methods include Strain Range Partitioning (SRP),[2] Damage Rate (DR),[3] Frequency Separation (FS),[4] and Strain Energy (SE).[5] Recent reviews of these methods are contained in Refs. 6 and 7. Development of these methods has been guided largely by results of relatively simple uniaxial experiments, and relatively little has been done to generalize them to more complicated multiaxial conditions. This report concerns an effort to extend SRP to more realistic design situations, and to improve the multiaxial formulation of linear damage summation.

* Research sponsored by the Office of Reactor Research and Technology, U.S. Department of Energy under contract W-7405-eng-26 with the Union Carbide Corporation.

2. Some Previous Work on Design Rules

Code Case N-47 (Ref. 1) contains multiaxial rules based on (Mises) equivalent stress and equivalent total strainrange. Because these quantities cannot distinguish between tensile and compressive hold periods in uniaxial tests, the procedure for accounting for creep-fatigue interaction is based on the worst case (tensile holds for most materials). Manson and Halford[8] used equivalent stress and equivalent inelastic strain concepts to extend SRP to multiaxial conditions, but they restricted their consideration to proportional loading paths. Their approach involves use of an auxiliary rule to attach algebraic signs to equivalent stress and strain. Lobitz and Nickell[9] suggested a somewhat different auxiliary rule and an incremental approach to calculation of partitioned strain ranges in SRP, removing the restriction to proportional paths.

3. Some Previous Work on Multiaxial Fatigue

All three multiaxial approaches mentioned in the preceding section employed Mises (or octahedral shear) stress and strain quantities. The literature contains numerous examples* of other quantities being used to correlate continuous-cycling fatigue data obtained under biaxial stress conditions. A reasonable question is whether one or more of these quantities might be more useful than octahedral shear in extending the proposed creep-fatigue methods to multiaxial conditions. A common feature of most methods, at least at their present stage of development, is that they are based on the inelastic portion of total strain. Their generalization to multiaxial conditions must for now also be based on inelastic strain, although in the long run, total strain may become a more useful basis.

In most cases, a rationalization based on existing evidence requires that one be prepared to contend with data obtained using different test methods, specimen geometry, surface finish, and definition of failure or to settle for a limited range of stress states. In the experiments reported by Parsons and Pascoe[10] involving direct biaxial straining of a cruciform specimen, the ratio of principal stresses in the plane of the specimen covered the full range from -1 to $+1$ (from pure shear to equal biaxial stress).

*See the reviews in Refs. 10 and 11 for examples.

These authors considered various theories of failure to correlate their data for a ferritic (QT 35) steel and an austenitic (AISI 304) steel and found that no one theory or strength criterion adequately accounted for the observed effects. However, a reasonable balance between simplicity and agreement with their data can be achieved by postulating a maximum inelastic principal strain range theory for principal stress ratios in the range −1 to 0 and a maximum inelastic shear strain range theory for principal stress ratios in the range 0 to 1. In the terminology of Brown and Miller,[11] this corresponds to the sum of inelastic shear and normal strain ranges on the planes of maximum inelastic shear strain range (*MS* planes) for case A (*MS* planes normal to the free surface) and the maximum inelastic shear strain range for case B (*MS* planes at 45° to the free surface).

Both of these criteria may be combined into a single expression for an equivalent or effective inelastic strain range:

$$\overline{\Delta\varepsilon'} = \frac{4}{3 + C}\left(\frac{1}{2}\Delta\gamma' + C\Delta\varepsilon'\right) = \Delta\varepsilon_0 \qquad (1)$$

with

$$C = 0 \text{ for } \phi = 45° \text{ and } C = 1 \text{ for } \phi = 90° ,$$

where $\Delta\gamma'$ is the maximum inelastic engineering shear strain range; $\Delta\varepsilon'$ is the inelastic strain range normal to the planes of $\Delta\gamma'$; $\Delta\varepsilon_0$ is the uniaxial inelastic strain range corresponding to a given number of cycles to failure, N_f; and ϕ is the angle between the *MS* planes and the free surface. The two-part criterion of Eq. (1) is plotted on the Γ-plane of Brown and Miller[11] in Fig. 1, and its relationship to Mohr's strain circles is indicated in Fig. 2. A plot of $\overline{\Delta\varepsilon'}$ vs N_f for the experiments of Parsons and Pascoe is shown in Fig. 3.

Unfortunately, Pascoe's test method has apparently been used only for proportional strain cycling. Although little is known* about the effects of nonproportional strain cycling, one cannot pretend that this sort of condition never occurs in realistic design situations. The available data are limited to out-of-phase axial and torsional (case A) strain cycling, with the most extensive set of experiments being those reported by Kanazawa, Miller, and Brown[12,13] on 1% Cr–Mo–V steel. Although the deformation

*See the review in Ref. 12.

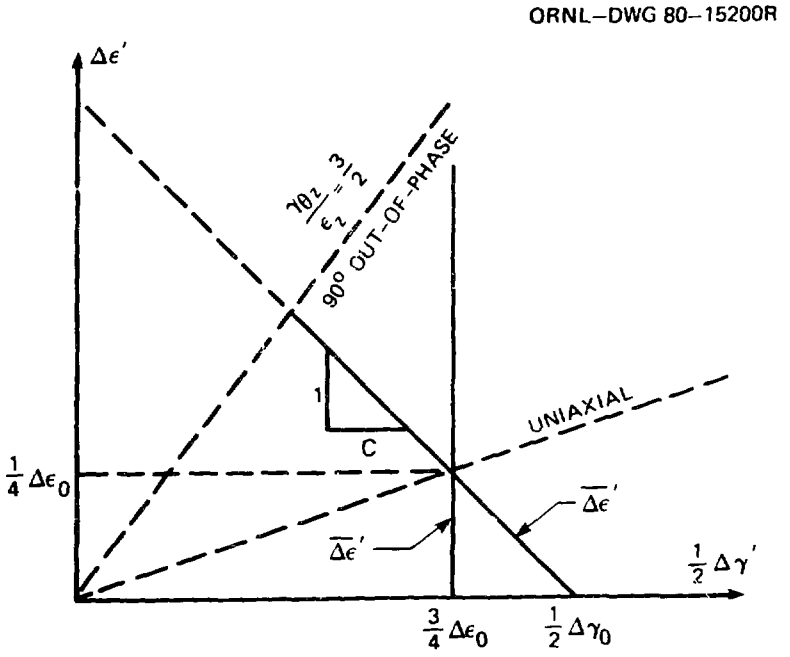

Fig. 1. Γ-plane plot of $\Delta\varepsilon'$ vs $\frac{1}{2}\Delta\gamma'$. Solid lines correspond to $\overline{\Delta\varepsilon'} = [4/(3 + C)](1/2\Delta\gamma' + C\Delta\varepsilon') = \Delta\varepsilon_0'$ corresponding to a given number of cycles to failure. Dashed lines correspond to $\Delta\varepsilon$ vs $1/2\Delta\gamma$ relationships for uniaxial loading and for the extreme case of out-of-phase sinusoidal, combined axial-torsional loading.

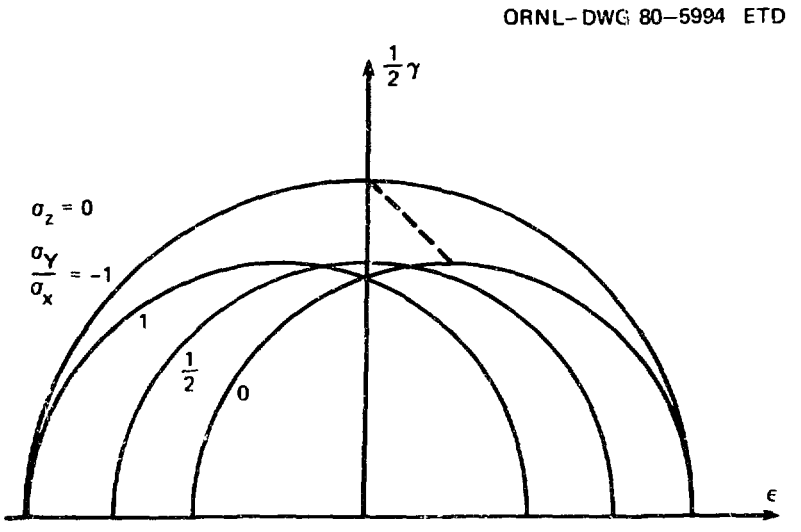

Fig. 2. Mohr's strain circles for several values of the biaxial stress ratio σ_y/σ_x. For values from -1 to 0, $\epsilon_{max} = 1/2\gamma' + \epsilon'$ is fixed, and for values from 0 to 1, $1/2\gamma'$ is fixed.

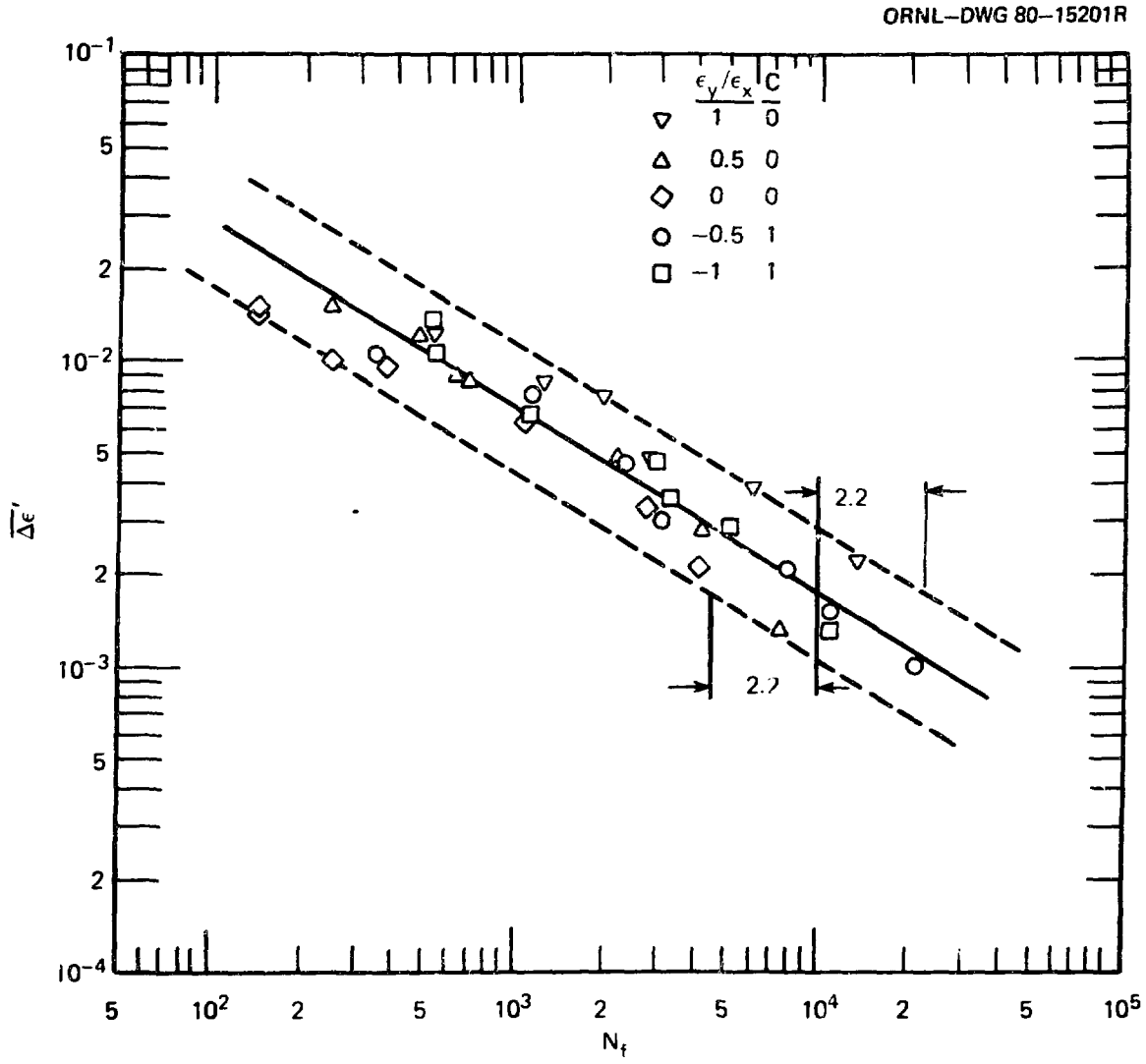

Fig. 3. Plot of $\Delta\epsilon' = [4/(3 + C)](1/2\Delta\gamma' + C\Delta\epsilon')$ vs N_f for tests conducted by M. W. Parsons on QT35 steel using direct biaxial straining in principal directions.

behavior[13] as a function of the phase angle between axial and torsional strain is quite complicated, Eq. (1) with $C = 1$ for $\phi = 90°$ nevertheless provides a reasonably good correlation of the failure behavior[12] as shown in Fig. 4. This is so even though the extreme values of γ' occurred at different times than those of ε'; that is, failure is not greatly influenced by the phase angle between γ' and ε', although for a given ratio of torsional to axial strain, the ratio of γ' to ε' depends on the phase angle between the axial and torsional strains.

All experiments discussed thus far were conducted at room temperature. At elevated temperatures, one might expect the effect of $\Delta\varepsilon'$ to be more severe because of its influence on grain boundary cavitation. Thus, larger values of C may be appropriate for elevated temperatures.

4. Multiaxial Fatigue at Elevated Temperature

In analyzing some recent results of multiaxial fatigue tests conducted at elevated temperature, an alternate definition of equivalent inelastic strain range based on the following relationship was employed.

$$\left(\frac{3\Delta\varepsilon_0}{2\Delta\gamma_0}\right)^{\beta}\left(\frac{2\Delta\gamma'}{3\Delta\varepsilon_0}\right)^{\beta} + \left[1 - \left(\frac{3\Delta\varepsilon_0}{2\Delta\gamma_0}\right)^{\beta}\right]\left(\frac{4\Delta\varepsilon'}{\Delta\varepsilon_0}\right)^{\beta} = 1 \,, \tag{2}$$

where $\Delta\gamma'$ and $\Delta\varepsilon'$, as in Eq. (1), are inelastic shear and normal components of strain range on the MS planes, $\Delta\varepsilon_0$ and $\Delta\gamma_0$ are inelastic strain ranges corresponding to a given N_f for tests conducted under uniaxial and pure shear conditions, respectively, and β is an empirical parameter. Equation (2) is somewhat similar to an expression employed by Brown and Miller[14] to describe multiaxial fatigue behavior of AISI 316 and 1% Cr–Mo–V steel at room and elevated temperatures in terms of total (elastic + plastic) strain amplitudes. In order to derive a useful expression for equivalent inelastic strain range $\overline{\Delta\varepsilon'}$ from Eq. (2) it is necessary to assume that the ratio $\Delta\gamma_0/\Delta\varepsilon_0$ and the parameter β are constants. This idealization was not employed by Brown and Miller in Ref. 14 but rather values of variables corresponding to $\Delta\gamma_0$, $\Delta\varepsilon_0$, and β were determined for several values of N_f. While greater accuracy may result from this procedure, it precludes a simple definition of $\overline{\Delta\varepsilon'}$, such as the following.

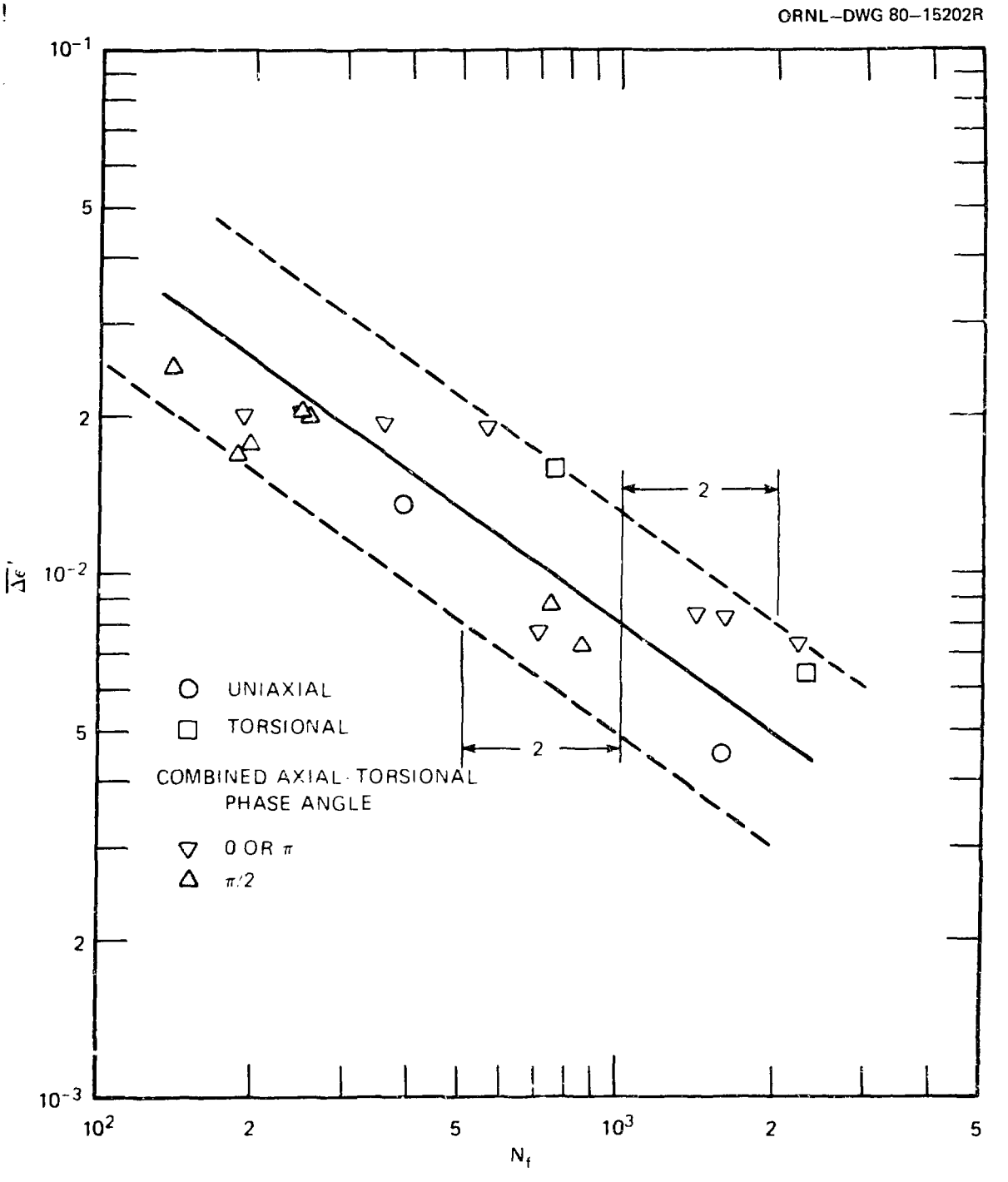

Fig. 4. Plot of $\Delta\varepsilon' = [4/(3 + C)](1/2\Delta\gamma' + C\Delta\varepsilon')$ vs N_f for tests conducted by K. Kanazawa on 1% Cr-Mo-V steel using out-of-phase combined axial-torsional straining.

$$\overline{\Delta\varepsilon'} = \frac{1}{B}\left[\left(\frac{2\Delta\gamma'}{3}\right)^{\beta} + (B^{\beta} - 1)(4\Delta\varepsilon')^{\beta}\right]^{1/\beta} , \tag{3}$$

where the constant B takes the place of $2\Delta\gamma_0/3\Delta\varepsilon_0$ in Eq. (2). Note also that Eq. (1) is a special case of Eq. (3) with $B = C/3 + 1$ and $\beta = 1$. For experiments conducted under combined axial-torsional stress conditions $(2\Delta\gamma'/3)^2 = (2\Delta\gamma/3)^2 + (\Delta\varepsilon)^2$ and $4\Delta\varepsilon' = \Delta\varepsilon$, where $\Delta\varepsilon$ and $\Delta\gamma$ are the inelastic axial and shear strain ranges respectively. For the special case of uniaxial stress, $\overline{\Delta\varepsilon'} = \Delta\varepsilon_0$. Equation (3) may be combined with the Coffin-Manson Law[15,16] $\Delta\varepsilon_0 = AN_f^{-\alpha}$, to give a relationship between N_f, $\Delta\gamma'$, and $\Delta\varepsilon'$. For purposes of comparison with the results of combined axial-torsional experiments the following form is appropriate

$$N_f = (AB)^{1/\alpha}/\{[(2\Delta\gamma/3)^2 + (\Delta\varepsilon)^2]^{\beta/2} + (B^{\beta} - 1)(\Delta\varepsilon)^{\beta}\}^{1/\alpha\beta} . \tag{4}$$

In this instance the usual (Mises) equivalent inelastic strain range becomes

$$\overline{\Delta\varepsilon} = [(\Delta\gamma)^2/3 + (\Delta\varepsilon)^2]^{1/2} = AN_f^{-\alpha} \tag{5}$$

or

$$N_f = (A)^{1/\alpha}/[(\Delta\gamma)^2/3 + (\Delta\varepsilon)^2]^{1/2\alpha} . \tag{6}$$

Inspection reveals that Eq. (5) is a special case of Eq. (3) with $B = 2/\sqrt{3}$ and $\beta = 2$. With selected values of B and β, Eq. (3) can be made to conform to a number of other fatigue failure criteria. A few examples are given in Table 1.

Table 1. Comparison of Eq. (3) with selected fatigue criteria

Fatigue criterion		B	β
Octahedral shear strain		$2/\sqrt{3}$	2
Maximum shear strain		1	1
Maximum principal strain		4/3	1
$\Delta\gamma^*$ (Lohr and Ellison[17])	Case A	2	1
	Case B	1	1

For a given material, optimum values of A, α, B, and β may be obtained by the method of least squares, provided that suitable test data are available. If desired, the estimation of A and α may be based on uniaxial data alone. For case A loading, however, B requires the addition of torsional data, and β combined axial-torsional data. For case B loading, pure shear with $\phi = 45°$ (2:1 biaxial stressing) takes the place of torsion.

Alternatively, A and α may be based on all of the data, torsional and combined axial-torsional as well as uniaxial, and B on combined axial-torsional as well as pure torsional. This approach was used in fitting Eqs. (4) and (6) to axial-torsional (Case A) data for AISI 304 and 2-1/4 Cr—1 Mo steel at 538°C (1000°F). The tests of AISI 304 were conducted at the Pennsylvania State University by S. Y. Zamrik[18] for Oak Ridge National Laboratory and the tests of 2-1/4 Cr—1 Mo steel were conducted at ORNL by K. C. Liu.[19]

By taking the logarithm, Eq. (6) can be put in a form suitable for standard linear regression analysis to obtain least-squares estimates of parameters related to A and α. However, from Eq. (4) $\log N_f$ is found to depend linearly on these parameters and nonlinearly on B and β. This class of problems is known as separable least-squares and the most efficient method of solution is the variable projection method.[20] In obtaining estimates of A, α, B, and β for Eqs. (4) and (6) individual observations were weighted so that the axial, torsional, and combined axial-torsional subsets of the data would all have the same influence on the residual sum of squares. The estimates are listed in Table 2 along with a scatter factor F. This factor is defined such that 95% of the observed lives N_f fall within the range $\hat{N}_f/F < N < \hat{N}_f F$ where $\hat{N}_f$ is the life estimated by either Eq. (4) or Eq. (6). This range corresponds, in other words, to plus or minus two standard errors on log of life. Examination of the values of F contained in Table 2 reveals that doubling the number of fitted constants in the life vs equivalent inelastic strain range relationship has more than halved the scatter about the expected value of N_f.

The results of the few exploratory tests used in this study are shown in Figs. 5-8 as log-log plots of $\overline{\Delta\varepsilon'}$ and $\overline{\Delta\varepsilon}$ vs N_f for each material. The solid lines in Figs. 5 and 7 correspond to Eq. (4) and those in Figs. 6

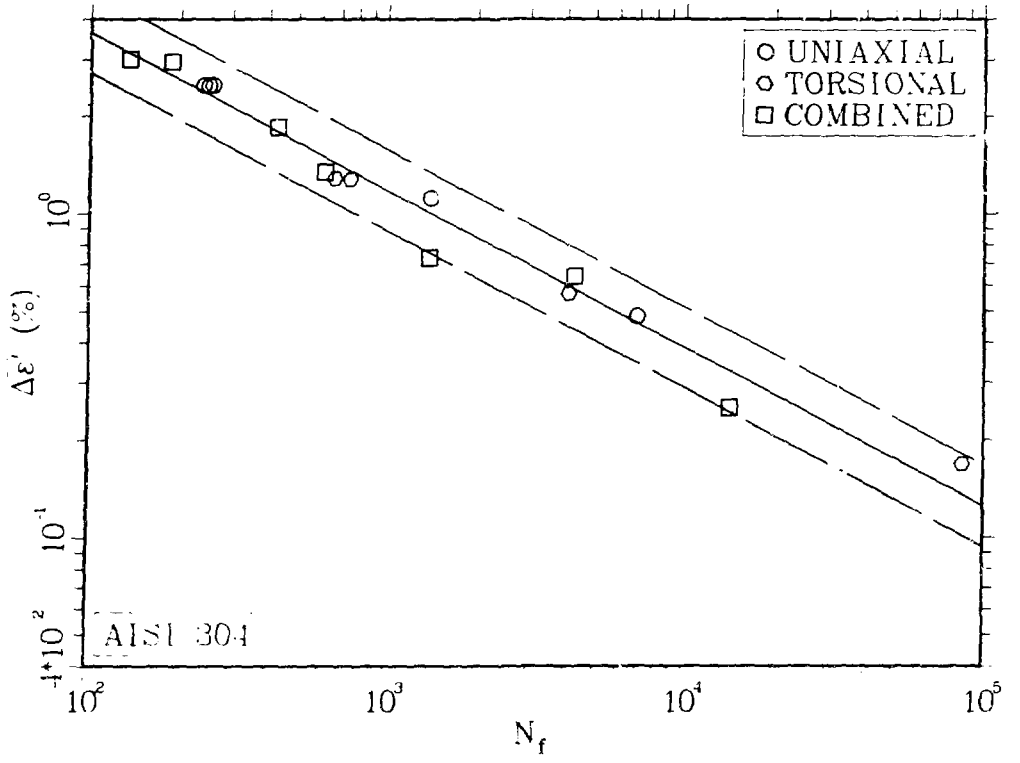

Fig. 5. Plot of $\overline{\Delta\varepsilon}' = [(2\Delta\gamma'/3)^{\beta} + (B^{\beta} - 1)(4\Delta\varepsilon')^{\beta}]^{1/\beta}/B$ vs N_f for axial-torsional strain cycling tests of AISI 304 at 538°C conducted by S. Y. Zamrik.

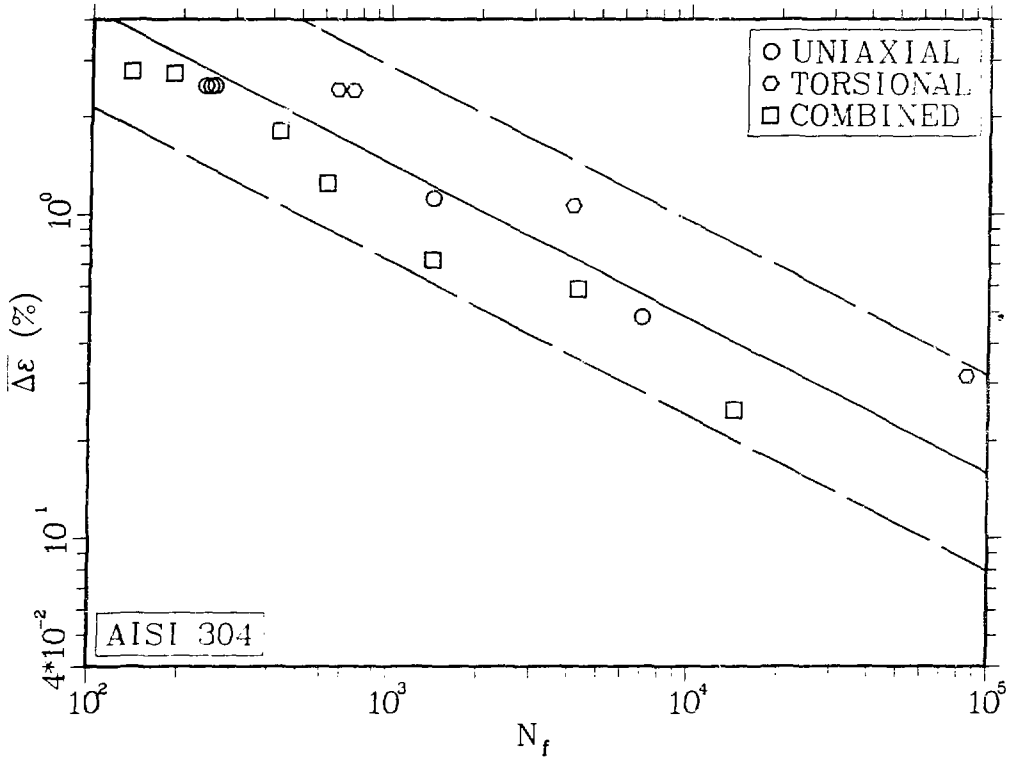

Fig. 6. Plot of (Mises) $\overline{\Delta\varepsilon}$ vs N_f for axial-torsional strain cycling tests of AISI 304 at 538°C conducted by S. Y. Zamrik.

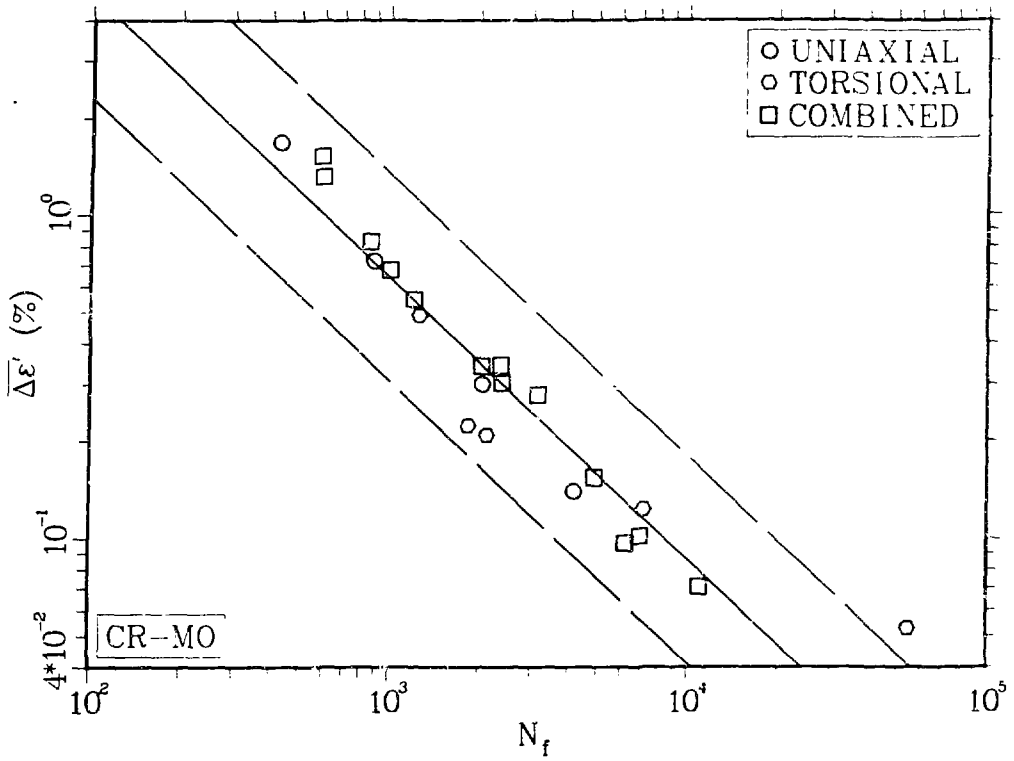

Fig. 7. Plot of $\overline{\Delta\varepsilon'} = [(2\Delta\gamma'/3)^{\beta} + (B^{\beta} - 1)(4\Delta\varepsilon')^{\beta}]^{1/\beta}/B$ vs for axial-torsional strain cycling tests of 2-1/4 Cr-1 Mo steel at 538°C conducted by K. C. Liu.

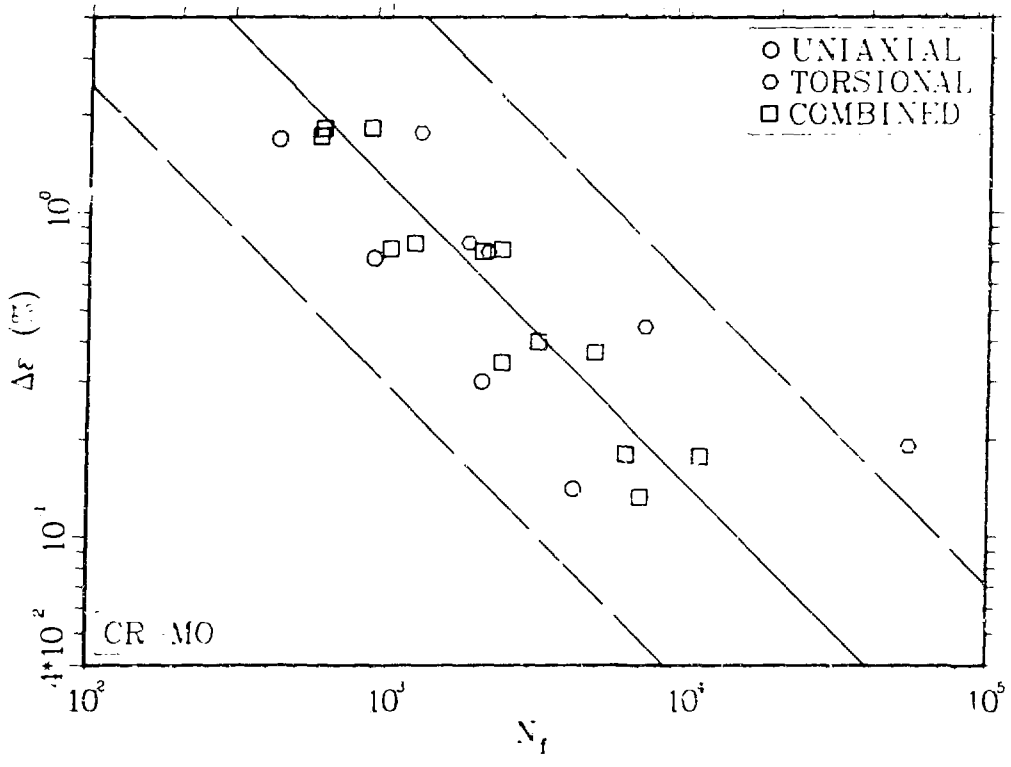

Fig. 8. Plot of (Mises) $\overline{\Delta\varepsilon}$ vs N_f for axial-torsional strain cycling tests of 2-1/4 Cr–1 Mo steel at 538°C conducted by K. C. Liu.

and 8 to Eq. (6) with the parameter values in Table 2. The scatter about these lines associated with the factor F is indicated by dashed lines. Figure 9 is a composite of Figs. 5 and 6 and shows the scatter band associated with Eq. (4) for AISI 304 as a pair of solid lines and the scatter band for Eq. (6) as a pair of dashed lines. Figure 10 is a composite of Figs. 7 and 8 showing each scatter band for 2-1/4 Cr–1 Mo steel. Again the improvement in data correlation due to inclusion in the model of fitted parameters B and β is evident.

Table 2. Results of least-squares fits of Eqs. (4) and (6) to axial-torsional (Case A) fatigue data at 538°C (1000°F)

Parameter	AISI 304		2-1/4 Cr–1 Mo	
	Eq. (4)	Eq. (6)	Eq. (4)	Eq. (6)
A	34.41	38.58	263.3	742.6
α	0.4880	0.4772	0.8709	0.9276
B	2.169	–	4.160	–
β	0.03560	–	2.450	–
F	1.81	4.28	2.32	4.67

Brown and Miller[11] refer to graphs of $\Delta\varepsilon'$ vs $1/2\Delta\gamma'$ for a given N_f as Γ-plane plots. Since they permit their parameters analogous to B and β to vary with N_f their Γ-plane plots of relationship like Eq. (2) are a group of curves differing in shape as well as size. By plotting the reduced values $(4\Delta\varepsilon'/\Delta\varepsilon_0)$ vs $(2\Delta\gamma'/3\Delta\varepsilon_0)$, and keeping B and β constant, a unique curve results from Eq. (2) depending only on the values chosen for B and β. Figure 11 shows such reduced Γ-plane plots for the fatigue criteria listed in Table 1, each a special case of Eq. (2), and for $B = 2$ with $\beta = 2$ and 1/2. Note that the uniaxial stress state is represented by a point with the coordinates (1,1) and pure shear by $(B,0)$.

The test results for AISI 304 are plotted on reduced Γ coordinates in Figs. 12 and 13, and the results for 2-1/4 Cr–1 Mo are plotted similarly in Figs. 14 and 15. In Figs. 12 and 14, A and α from Table 2 for Eq. (4) were used in the Coffin-Manson Law to calculate the uniaxial strain range $\Delta\varepsilon_0'$ corresponding to the observed value of N_f in each test. In Figs. 13

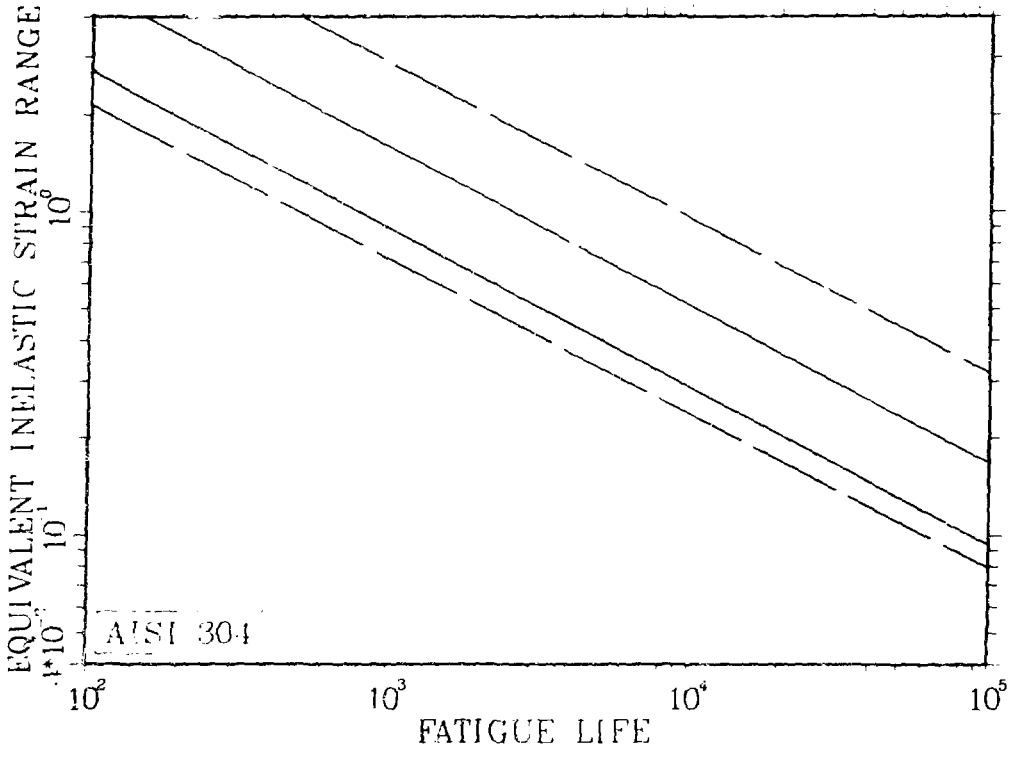

Fig. 9. Comparisons of scatter bands for AISI 304 at 538°C resulting from two definitions of equivalent inelastic strain range. Solid lines correspond to $\overline{\Delta\varepsilon'}$ and dashed lines to $\overline{\Delta\varepsilon}$.

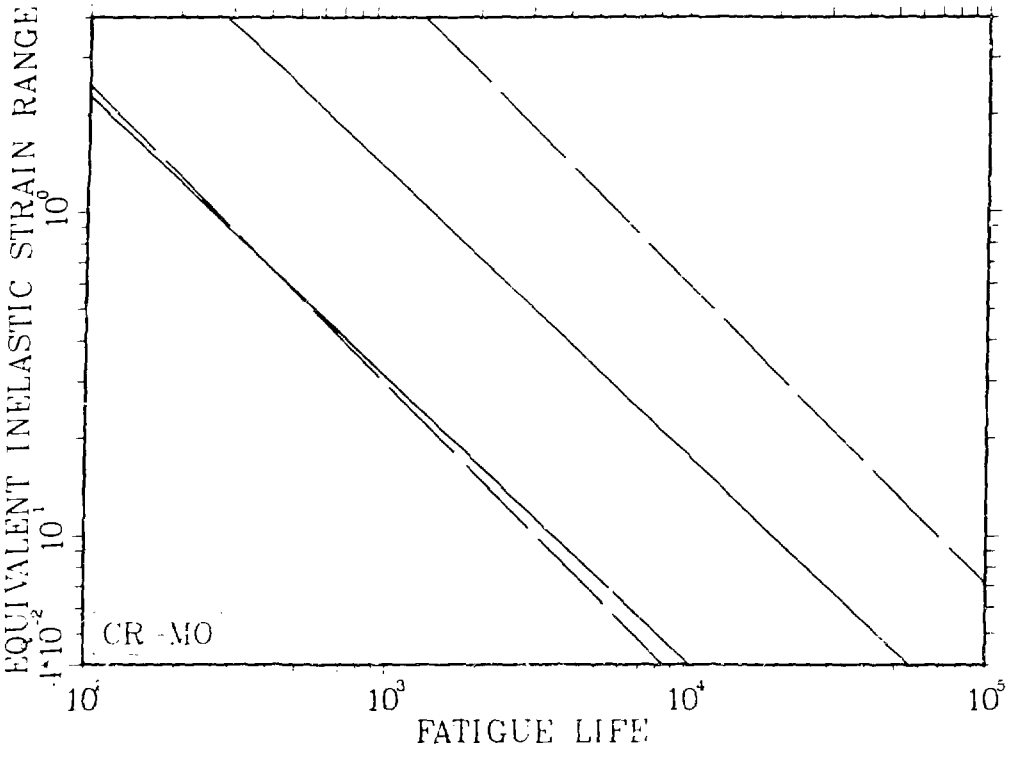

Fig. 10. Comparisons of scatter bands for 2-1/4 Cr–1 Mo steel at 538°C resulting from two definitions of equivalent inelastic strain range. Solid lines correspond to $\overline{\Delta\varepsilon'}$ and dashed lines to $\overline{\Delta\varepsilon}$.

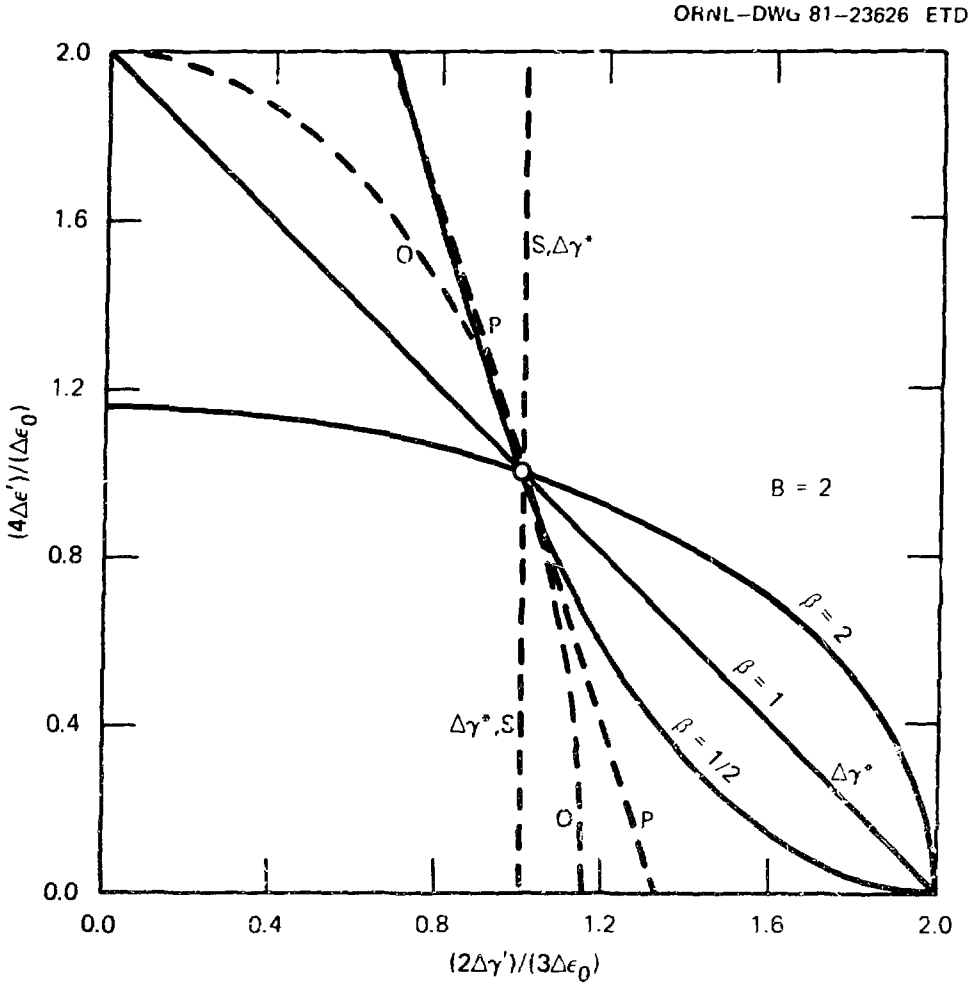

Fig. 11. Reduced Γ-plane plot of $(4\Delta\varepsilon')/(\Delta\varepsilon_0)$ vs $(2\Delta\gamma')/(3\Delta\epsilon_0)$ for a number of different fatigue criteria. Solid lines correspond to $\overline{\Delta\varepsilon'} = \Delta\varepsilon_0$ for indicated values of B and β. Dashed lines correspond to simpler criteria. Curve O is for the Octahedral Shear Strain Criterion, S for Maximum Shear Strain, and P for Maximum Principal Strain. $\Delta\gamma^*$ stands for the Criterion of Lohr and Ellison.

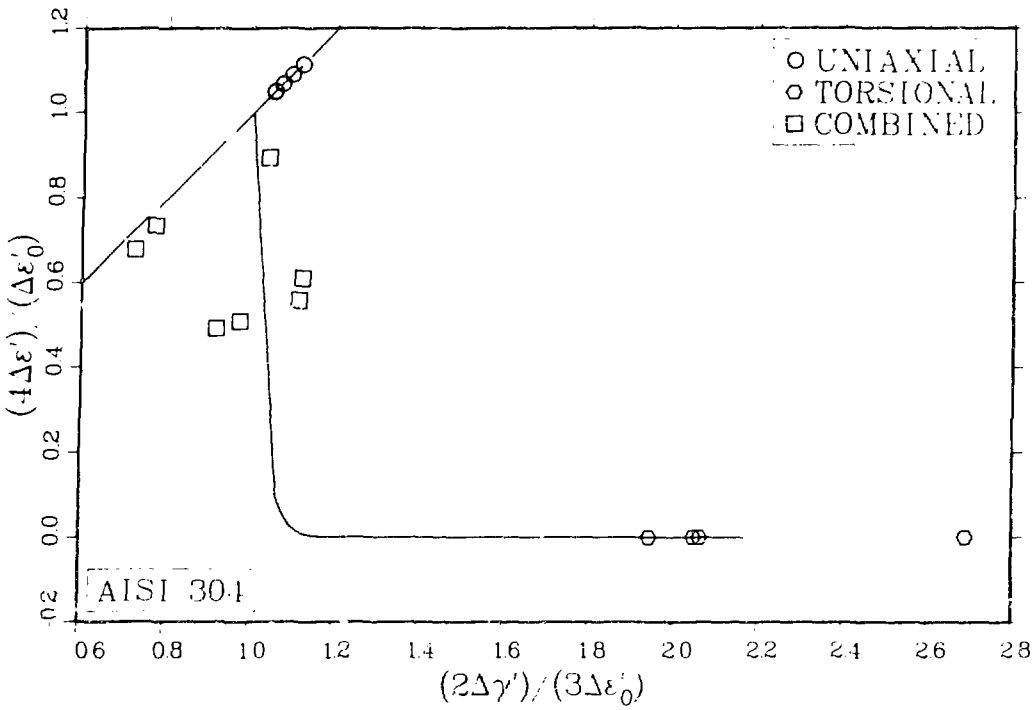

Fig. 12. Reduced Γ-plane plot for AISI 304 at 538°C. Values of A and α from Eq. (4) used to estimate inelastic axial strain range $\Delta\varepsilon'_0$ for observed values of N_f.

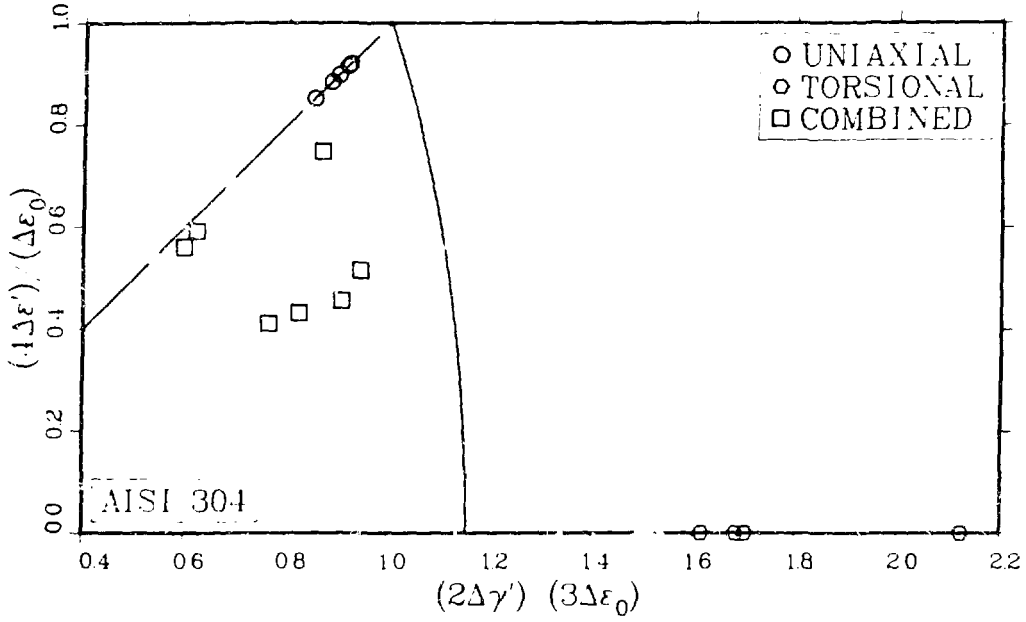

Fig. 13. Reduced Γ-plane plot for AISI 304 at 538°C. Values of A and α from Eq. (6) used to estimate inelastic axial strain range $\Delta\varepsilon_0'$ for observed values of N_f.

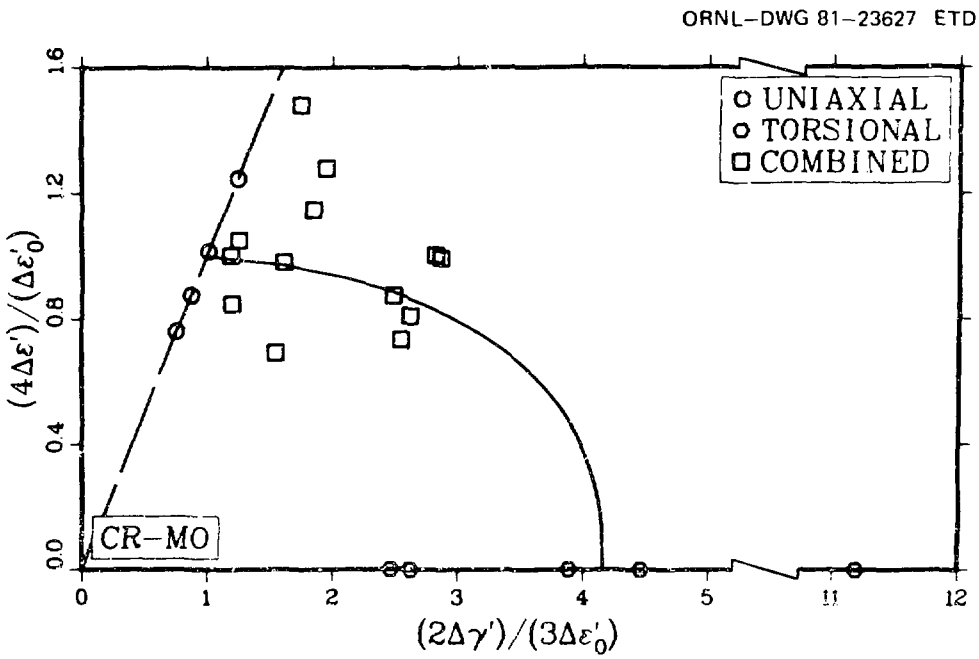

Fig. 14. Reduced Γ-plane plto for 2-1/4 Cr–1 Mo steel at 538°C. Values of A and α from Eq. (4) used to estimate inelastic axial strain range $\Delta\varepsilon'_0$ for observed values of N_f.

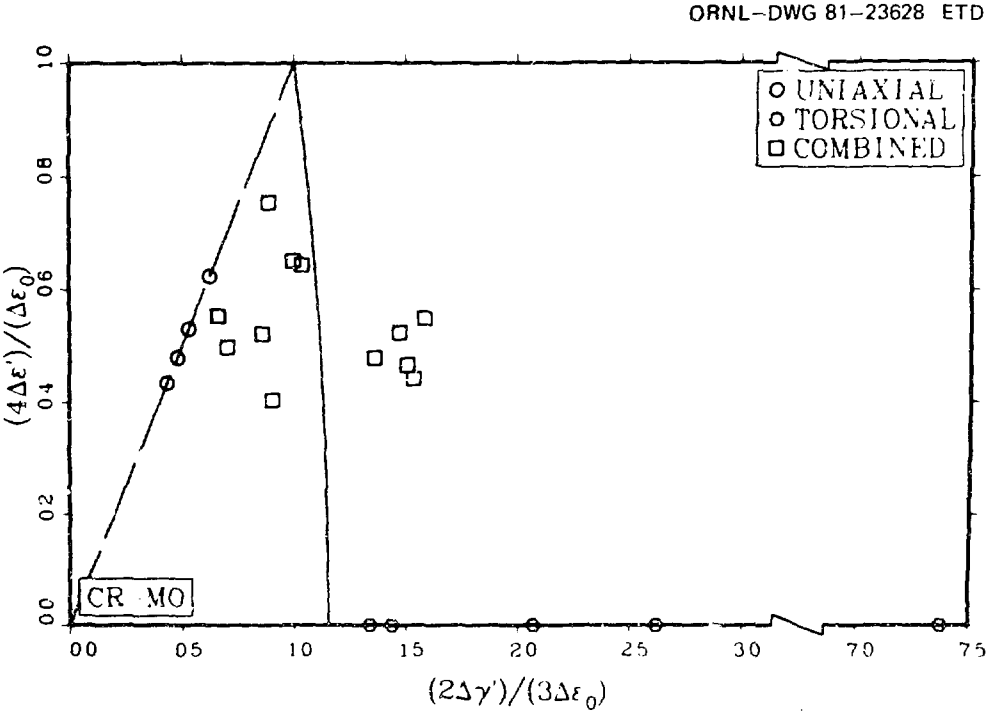

Fig. 15. Reduced Γ-plane plot for 2-1/4 Cr–1 Mo steel at 538°C. Values of A and α from Eq. (6) used to estimate inelastic axial strain range $\Delta\varepsilon_0'$ for observed values of N_f.

and 15, A and α from Table 2 for Eq. (6) were used to calculate $\Delta\varepsilon_0$. Similarly the solid curves plotted in Figs. 12 and 14 represent $\overline{\Delta\varepsilon'} = \Delta\varepsilon_0'$ from Eq. (3) with the fitted values of B and β from Table 2 and those in Figs. 13 and 15 represent $\overline{\Delta\varepsilon} = \Delta\varepsilon_0$, from Eq. (5) or Eq. (3) with the fixed values of B and β corresponding to the Octahedral Shear Criterion in Table 1. The solid curves in Figs. 12-15 pass through the points with coordinates (1,1) and (B,0) as they are constrained to do. However, the test data corresponding to uniaxial stress are spread out along the straight line passing through (0,0) and (1,1), and those corresponding to pure shear are spread out along the abscissa. The combined axial-torsional data tend to lie in radial bands. All of this variability is due both to the inherent scatter in N_f and to the lack of perfect agreement with the assumptions made concerning the values of B and β. Once again there is noticably better agreement between the data and curves for Eq. (4) than for Eq. (6).

5. Calculation of *MS* Components

Fatigue cracking usually originates at a free surface. If the components of strain at a point on the free surface are defined with respect to a Cartesian coordinate system oriented with its z-axis normal to the surface, then $\gamma_{xz} = \gamma_{yz} = 0$ and

$$\Delta\gamma' = \max_{m,n}\left(\gamma_3^{mn},\ \gamma_2^{mn},\ \gamma_1^{mn}\right) , \tag{7}$$

where

$$\gamma_3^{mn} = \left[\left(\varepsilon_x^{mn} - \varepsilon_y^{mn}\right)^2 + \left(\gamma_{xy}^{mn}\right)^2\right]^{1/2} ,$$

$$\gamma_2^{mn}, \gamma_1^{mn} = \frac{1}{2}\left|\varepsilon_x^{mn} + \varepsilon_y^{mn} - 2\varepsilon_z^{mn} \pm \gamma_3^{mn}\right| , \tag{8}$$

$\varepsilon_x(t_n)$, for instance, is the inelastic normal strain in the x-direction at time t_n, and $\varepsilon_x^{mn} = \varepsilon_x(t_n) - \varepsilon_x(t_m)$. Denoting as t_M and t_N the times corresponding to the maximum in Eq. (7), the *MS* planes are normal to the free surface (case A) if γ_3^{MN} is the largest of the three principal shear strain differences γ_3^{MN}, γ_2^{MN}, and γ_1^{MN}, and the *MS* planes are at 45° to the free surface (case B) if γ_2^{MN} or γ_1^{MN} is the largest. For case A

$$\Delta\varepsilon' = \max_{k,\ell} \frac{1}{2}\left\{\varepsilon_x^{k\ell} + \varepsilon_y^{k\ell} \pm \left[\gamma_{xy}^{k\ell}\left(\varepsilon_x^{MN} - \varepsilon_y^{MN}\right) - \left(\varepsilon_x^{k\ell} - \varepsilon_y^{k\ell}\right)\gamma_{xy}^{MN}\right]/\gamma_3^{MN}\right\} , \quad (9)$$

where the ± signs correspond to mutually perpendicular planes. For case B

$$\Delta\varepsilon' = \max_{k,\ell} \frac{1}{4}\left\{\varepsilon_x^{k\ell} + \varepsilon_y^{k\ell} + 2\varepsilon_z^{k\ell} \pm \left[\left(\varepsilon_x^{k\ell} - \varepsilon_y^{k\ell}\right)\left(\varepsilon_x^{MN} - \varepsilon_y^{MN}\right) + \gamma_{xy}^{k\ell}\gamma_{xy}^{MN}\right]/\gamma_3^{MN}\right\} , \quad (10)$$

where the correct sign to use is known from Eq. (8). If the times corresponding to the maximum in Eq. (9) or (10) are denoted t_K and t_L, then for in-phase cycling $t_K = t_M$, $t_L = t_N$, and the term with the ± sign is equal to zero in Eq. (9) and to γ_3^{MN} in Eq. (10).

The *MS* components of inelastic strain rate, which would be expected to play a role in time-dependent fatigue methods such as SRP and DI, are for case A

$$\begin{aligned} \dot{\gamma}' &= \left[\left(\dot{\varepsilon}_x - \dot{\varepsilon}_y\right)\left(\varepsilon_x^{MN} - \varepsilon_y^{MN}\right) + \dot{\gamma}_{xy}\gamma_{xy}^{MN}\right]/\gamma_3^{MN} , \\ \dot{\varepsilon}' &= \frac{1}{2}\left\{\dot{\varepsilon}_x + \dot{\varepsilon}_y \pm \left[\dot{\gamma}_{xy}\left(\varepsilon_x^{MN} - \varepsilon_y^{MN}\right) - \left(\dot{\varepsilon}_x - \dot{\varepsilon}_y\right)\gamma_{xy}^{MN}\right]/\gamma_3^{MN}\right\} , \end{aligned} \quad (11)$$

where the correct sign to use in the second equation is known from Eq. (9), and for case B

$$\begin{aligned} \dot{\gamma}' &= \frac{1}{4}\left(\dot{\varepsilon}_x + \dot{\varepsilon}_y - 2\dot{\varepsilon}_z \pm \dot{\gamma}_3\right) , \\ \dot{\varepsilon}' &= \frac{1}{4}\left(\dot{\varepsilon}_x + \dot{\varepsilon}_y + 2\dot{\varepsilon}_z \pm \dot{\gamma}_3\right) , \end{aligned} \quad (12)$$

where the correct sign to use in both equations is known from Eq. (8).

6. Strain Range Partitioning

Before proceeding to the extension of SRP to multiaxial conditions, a concise statement of this method under uniaxial conditions will be presented, including a brief discussion of possible effects of nonrepetitive or random cycling.

In SRP, inelastic strain is presumed to consist of two kinds of strain, called creep and plasticity (although these terms do not refer to time-dependent and time-independent inelastic strain, respectively). In

more recently published versions,[8] creep refers to secondary or steady-state creep only, and primary or transient creep is considered part of plasticity. Thus, in the following presentation, $\dot{\varepsilon}_c\ (\sigma, T)$ is the minimum strain rate or secondary creep rate in a constant-stress σ, constant-temperature T, creep test.

Adopting the "rain flow" method[21,22] of cycle counting seems appropriate. Therefore, in Fig. 16, times t_j, t_k, and t_l correspond to successive extremes in a complete cycle of inelastic strain which, in this illustration, is viewed as an interruption in a period of steadily increasing inelastic strain. The inelastic strain range is:

$$\Delta\varepsilon = \int_{t_j}^{t_k} |\dot{\varepsilon}|dt = \int_{t_k}^{t_l} |\dot{\varepsilon}|dt \ ,$$

where $\dot{\varepsilon}$ is the inelastic strain rate. This is partitioned into four basic strain ranges as follows:

$$\Delta\varepsilon_{cc} = \min\left(\int_{t_j}^{t_k} |\dot{\varepsilon}_c|dt, \int_{t_k}^{t_l} |\dot{\varepsilon}_c|dt\right) \ ,$$

$$\Delta\varepsilon_{pp} = \min\left(\int_{t_j}^{t_k} |\dot{\varepsilon} - \dot{\varepsilon}_c|dt, \int_{t_k}^{t_l} |\dot{\varepsilon} - \dot{\varepsilon}_c|dt\right) \ , \qquad (13)$$

$$\Delta\varepsilon_{cp} = \Delta\varepsilon - \Delta\varepsilon_{cc} - \Delta\varepsilon_{pp} \ ,$$

and

$$\Delta\varepsilon_{pc} = 0 \ ,$$

provided that the creep strain accumulated during the cycle's increasing inelastic strain portion exceeds the absolute value of the creep strain accumulated during the cycle's decreasing inelastic strain portion. Otherwise, the values of $\Delta\varepsilon_{cp}$ and $\Delta\varepsilon_{pc}$ are interchanged. From the above definitions, it is clear that $\Delta\varepsilon_{cp}$, for instance, represents the amount of positive creep strain that is reversed by negative plastic strain. Associated with each of the four basic strain cycles, Eq. (13) is a life relationship of the Coffin-Manson form, and for a combination of the basic cycles, a weighted average of the four basic damage or reciprocal of life values is calculated.

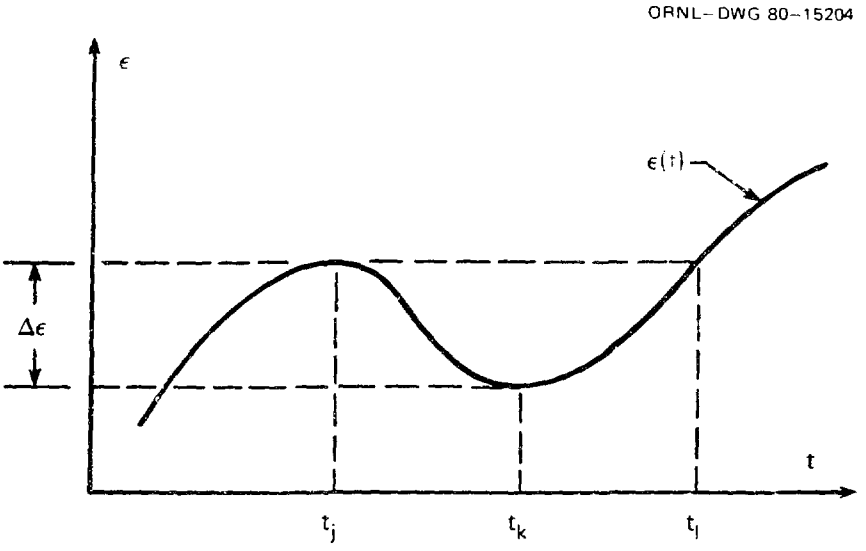

Fig. 16. Schematic plot of inelastic strain vs time. $\varepsilon(t)$ for $t_j \leqq t \leqq t_l$ constitutes a closed cycle.

The explicit repetition of similar equations and terms can be avoided if a unique value of an index k is used to denote each of the four basic types of strain cycle defined in SRP. One way of doing this is as follows:

k:	1	2	3	4
cycle:	*pp*	*pc*	*cp*	*cc*

where $k = 2$, for instance, stands for *pc* or plasticity reversed by creep. The four basic damage vs inelastic strain range relations may then be written as

$$1/N_k = (\Delta\varepsilon/A_k)^{1/\alpha_k} , \tag{14}$$

where k is understood to vary from 1 to 4. Weights or strain range fractions are defined as

$$F_k = \Delta\varepsilon_k/\Delta\varepsilon , \tag{15}$$

for which $\sum_{k=1}^{4} F_k = 1$. The combined estimate of damage per cycle is given by the so-called interaction damage rule as

$$\frac{1}{N_f} = \sum_{k=1}^{4} \frac{F_k}{N_k} . \tag{16}$$

where N_f is the estimated life if the same cycle is repeated until failure (initiation of a macrocrack) occurs. If the strain history consists of a sequence of different cycles, damage is summed cycle after cycle until the total damage reaches unity. For a strain history containing a ratchetting sequence consisting of a half-cycle of steadily increasing strain interrupted by several complete strain cycles, the assumption that the half-cycle is completed by a rapid reversal to include its effect in the running damage estimate seems reasonable.

Of the four basic strain cycles, either the *cp* cycle or the *pc* cycle seems to be the most damaging for most materials. This is sometimes attributed to internal ratchetting, meaning that when the same cycle is repeated, a large internal creep strain accumulates in one direction of straining and a large internal plastic strain accumulates in the opposite

direction. In a complex strain history, a *ep* cycle might be followed shortly by a *pe* cycle. The effect of this sequence might not be much different from a sequence consisting of a *ee* cycle and a *pp* cycle (Manson[23] calls this "strian range conversion"), implying that a cycle-by-cycle damage summation procedure might overestimate damage.

To extend SRP to more realistic design situations, defining what constitutes a multiaxial strain cycle is necessary. The multiaxial fatigue criterion of Eq. (3) is based in part on the experimental observations of Kanazawa, Miller, and Brown.[12] In their experiments, the strain trajectory, or the locus of strain components vs time, was an ellipse in four-dimensional strain space. This trajectory could be altered in several ways which appear to have practical significance. First, the ellipse could change in both size and shape with time. This is a multiaxial generalization of variable amplitude cycling. Second, the ellipse could move along a curved path in strain space. This corresponds to variable mean strain. Third, in a realistic design situation, the calculated strain trajectory would probably not be as smooth as the distorted corkscrew described in the two previous statements.

An extension of SRP will now be presented which is directly applicable to the elliptical strain trajectory mentioned above (or to piecewise linear trajectories inscribed within the ellipse). Further extension to the distorted corkscrew trajectory may conceivably be accomplished through application of the principles underlying the rain-flow cycle counting method.

If the damage process involves the interaction of fatigue cracks and creep cavities, failure must still originate at the free surface. The procedure discussed earlier in connection with Eqs. (7) through (10) for continuous cycling may again be used to determine an equivalent inelastic strain range $\overline{\Delta\varepsilon}$ in terms of the inelastic shear and normal strains acting on the critical *MS* plane. With the orientation of this place established, $\Delta\varepsilon'$ and $\Delta\gamma'$ may each be partitioned into four basic strain ranges, using the strain rates given in Eqs. (11) and (12) and similar expressions for the secondary creep rates associated with the *MS* plane. The normal strain range $\Delta\varepsilon'$ may be partitioned as follows:

$$\Delta\varepsilon'_{cc} = \min\left(\int_{t_j}^{t_k} |\dot{\varepsilon}'_c|dt,\ \int_{t_k}^{t_l} |\dot{\varepsilon}'_c|dt\right) ,$$

$$\Delta\varepsilon'_{pp} = \min\left(\int_{t_j}^{t_k} |\dot{\varepsilon}' - \dot{\varepsilon}'_c|dt,\ \int_{t_k}^{t_l} |\dot{\varepsilon}' - \dot{\varepsilon}'_c|dt\right) , \qquad (17)$$

$$\Delta\varepsilon'_{cp} = \Delta\varepsilon' - \Delta\varepsilon'_{cc} - \Delta\varepsilon'_{pp} ,$$

and

$$\Delta\varepsilon'_{pc} = 0 ,$$

provided that the creep strain accumulated during the tensile portion of the ε' cycle exceeds the absolute value of the creep strain accumulated during the compressive portion. Otherwise, the values of $\Delta\varepsilon'_{cp}$ and $\Delta\varepsilon'_{pc}$ are interchanged. The times t_j, t_k, and t_l, which correspond to extremes of the ε' cycle, are known from Eq. (9). $\Delta\gamma'$ may be partitioned in a similar manner, except that a convenient basis for choosing between *cp* and *pc* as the designation for the mixed shear strain range seems to be consistency with the designation of the mixed normal strain range. Assuming that the damage vs basic equivalent strain range relationships are of the form:

$$\frac{1}{N_k} = \left(\frac{\overline{\Delta\varepsilon'}}{A_k}\right)^{1/\alpha_k} = \frac{\left[(2\Delta\gamma'/3)^{\beta_k} + (B_k^{\beta_k} - 1)(4\Delta\varepsilon')^{\beta_k}\right]^{1/(\alpha_k\beta_k)}}{(A_k B_k)^{1/\alpha_k}} , \qquad (18)$$

which is analogous to Eq. (14) and is based on Eq. (3), and the equivalent strain range fractions are

$$F_k = \frac{\overline{\Delta\varepsilon'_k}}{\overline{\Delta\varepsilon'}} = \left[\frac{(2\Delta\varepsilon'_k/3)^{\beta} + (B^{\beta} - 1)(4\Delta\varepsilon'_k)^{\beta}}{(2\Delta\gamma'/3)^{\beta} + (B^{\beta} - 1)(4\Delta\varepsilon')^{\beta}}\right]^{1/\beta} , \qquad (19)$$

which is analogous to Eq. (15), then the interaction damage rule, Eq. (16) carries over to multiaxial stress-strain conditions. Note that for proportional stressing $F_k = \Delta\gamma'_k/\Delta\gamma' = \Delta\varepsilon'_k/\Delta\varepsilon'$ and the parameters B and β in Eq. (19) relate only to nonproportional stressing which is nevertheless a condition expected to be encountered in service. Note also that the set of eight parameters B_k and β_k in Eq. (18) might take on different values

for case A and case B loading. For Case A *pp* cycling, B_1 and β_1 for AISI 304 and 2-1/4 Cr–1 Mo steel are as given in Table 2. For other conditions little is known, although some evidence[10] suggests that for Case B, B_1 and β_1 may each be about unity. The determination of most of these parameters and the assessment of this approach must await the results of additional multiaxial testing. This testing is currently underway at ORNL, but at a pace constrained by limited resources.

7. Linear Damage Summation

It was Taira[24] who apparently first suggested that time and cycle fractions be added together to estimate damage, and this approach was subsequently adopted in ASME Code Case N-47 (Ref. 1) for the design of certain nuclear power plant components intended for elevated temperature service. The multiaxial formulation of this concept is normally based on the usual Mises equivalent stress and strain quantities. The evidence presented earlier in this report indicates that a definition of equivalent strain range based on the shear and normal components of strain range on the planes of maximum shear strain range would provide improved estimates of fatigue damage. An analogous definition of equivalent stress based on shear and normal components of stress on the planes of maximum shear stress might provide improved estimates of creep damage. The limited evidence[25] available for AISI 304 at 593°C (1100°F) includes one creep rupture test of a tube in pure torsion. Unlike tests in the first quadrant of biaxial principal stress space, this test can distinguish between the maximum principal stress criterion and the maximum shear stress criterion. The result was in-between the two criteria but much closer to the former than say the Mises criterion would suggest. While such limited evidence does not provide an adequate basis for the development of an emphirical strength criterion, it does support the contention that improvements to the multiaxial formulation of Linear Damage Summation are possible once an adequate data base is available.

8. Conclusions

1. The definition of equivalent inelastic strain range $\overline{\Delta\varepsilon'}$ given in Eq. (3) together with empirically determined values for the parameters B and β can provide a more precise estimate of fatigue damage under multiaxial stress and strain conditions than the usual (Mises) definition of equivalent inelastic strain range as well as other definitions based on simple classical strength criteria. This has been demonstrated for AISI 304 and 2-1/4 Cr–1 Mo steel in axial-torsional strain cycling tests at 538°C (1000°F).

2. The $\overline{\Delta\varepsilon'}$ concept can be used to generalize Strain Range Partitioning to complicated multiaxial conditions, however, additional multiaxial test data is required for the determination of certain parameters employed in this generalization.

3. Improvements to the multiaxial formulation of Linear Damage Summation appear to be possible with estimates of fatigue damage based on $\overline{\Delta\varepsilon'}$ and estimates of creep damage based on an analogous approach involving components of stress on the planes of maximum shear stress. Additional multiaxial test data are required to develop this approach for estimating creep damage.

4. Assessment of the validity of these approaches requires further multiaxial creep-fatigue testing.

References

1. "Case N-47-20," Cases of ASME Boiler and Pressure Vessel Code, American Society of Mechanical Engineers, New York, May 1981.

2. S. S. Manson, G. R. Halford, and M. H. Hirshberg, "Creep-Fatigue Analysis by Strainrange Partitioning," *Design for Elevated Temperature Environment*, American Society of Mechanical Engineers, New York, 1971, pp. 12-28.

3. S. Majumdar and P. S. Maiya, "A Damage Equation for Creep-Fatigue Interaction," pp. 323-35 in *1976 ASME-MPC Symposium on Creep-Fatigue Interaction*, MPC-3, American Society of Mechanical Engineers, New York, 1976.

4. L. F. Coffin, Jr., "The Concept of Frequency Separation in Life Prediction for Time-Dependent Fatigue," pp. 349-63 in *1976 ASME-MPC Symposium on Creep-Fatigue Interaction*, MPC-3, American Society of Mechanical Engineers, New York, 1976.

5. J. T. Fong, "Energy Approach for Creep-Fatigue Interactions in Metals at High Temperatures," *J. Pres. Ves. Tech.* 97, 214-322 (August 1975).

6. S. S. Manson, "A Critical Review of Predictive Methods for Treatment of Time-Dependent Metal Fatigue at High Temperatures." *Pressure Vessel and Piping Design Technology — A Decade of Progress*, American Society of Mechanical Engineers, New York, 1982.

7. S. Majumdar, P. S. Maiya, and M. K. Booker, *Time-Dependent Fatigue Behavior and Life Predictions for Type 304 Stainless Steel and 2-1/4 Cr—1 Mo Steel*, ANL-81-20, Argonne National Laboratory, 1981.

8. S. S. Manson and G. R. Halford, "Treatment of Multiaxial Creep-Fatigue by Strainrange Partitioning," pp. 299-322 in *1976 ASME-MPC Symposium on Creep-Fatigue Interaction*, MPC-3, American Society of Mechanical Engineers, New York, 1976.

9. D. W. Lobitz and R. E. Nickell, "Creep-Fatigue Damage Under Multiaxial Conditions," *Structural Mechanics in Reactor Technology (IV)*, L413, 1977.

10. M. W. Parsons and K. J. Pascoe, "Low-Cycle Fatigue Under Biaxial Stress," *Proc. Instn. Mechanical Engineers* 188 61/74, 657-71 (1974).

11. M. W. Brown and K. J. Miller, "A Theory for Fatigue Failure Under Multiaxial Stress-Strain Conditions," *Proc. Instn. Mechanical Engineers* 187 65/73, 745-55; also discussion, D229-44 (1973).

12. K. Kanazawa, K. J. Miller, and M. W. Brown, "Low-Cycle Fatigue Under Out-of-Phase Loading Conditions," *Trans. American Society of Mechanical Engineers, J. Eng. Mater. Tech.*, 99(H), 222-28 (July 1977).

13. K. Kanazawa, K. J. Miller, and M. W. Brown, "Cyclic Deformation of 1% Cr-Mo-V Steel Under Out-of-Phase Loads," *Fat. Engr. Mater. Struct.* 2, 217-28 (1980).

14. M. W. Brown and K. J. Miller, "High Temperature Low Cycle Biaxial Fatigue of Two Steels," *Fat. Engr. Mater. Struct.* 1, 217-29 (1979).

15. L. F. Coffin, Jr., "A Study of the Effects of Cyclic Thermal Stresses on a Ductile Metal," *Trans. American Society of Mechanical Engineers*, 76, 931-50 (1954).

16. S. S. Manson, *Behavior of Materials Under Conditions of Thermal Stress*, NACA TN-2933, National Advisory Committee for Aeronautics, 1953.

17. R. D. Lohr and E. G. Ellison, "A Simple Theory for Low Cycle Multiaxial Fatigue," *Fat. Engr. Mater. Struct.* 3, 1-17 (1980).

18. S. Y. Zamrik, "Effect of Biaxiality in Creep-Fatigue at Elevated Temperature," *High-Temperature Structural Design Program Prog. Rep. Dec. 31, 1978*, ORNL-5540, pp. 149-60.

19. K. C. Liu, "Biaxial Fatigue Testing of Annealed 2-1/4 Cr–1 Mo Steel at 538°C (1000°F)," *High-Temperature Structural Design Program Prog. Rep. June 30, 1981*, ORNL-5794 (in press).

20. G. H. Golub and V. Pereyia, "The Differentiation of Pseudo-Inverses and Nonlinear Least Squares Problems Whose Variables Separate," *SIAM J. Numer. Anal.* 10, 413-32 (1973).

21. M. Matsuishi and T. Endo, *Fatigue of Metals Subjected to Varying Stress*, Japan Society of Mechanical Engineers, Fukuoka, Japan, March 1968.

22. N. E. Dowling, "Fatigue Failure Predictions for Complicated Stress-Strain Histories," *J. Materials* 7(1), 71-87 (March 1972).

23. S. S. Manson, "Some Useful Concepts for the Designer Regarding Cumulative Fatigue Damage at Elevated Temperatures," Third International Conference on Mechanical Behavior of Materials, University of Cambridge, U.K. (August 1979).

24. S. Taira, "Lifetime of Structures Subjected to Varying Load and Temperature," pp. 96-124 in *Creep in Structures*, N. J. Hoff, ed., Academic Press, New York, 1962.

25. R. L. Huddleston, "Assessment of Torsional Creep-Rupture Data," *High-Temperature Structural Design Program Prog. Rep. June 30, 1980*, ORNL-5683, pp. 57-63.